Physics Letters A ••• (••••) •••–•••

Contents lists available at ScienceDirect

Physics Letters A

www.elsevier.com/locate/pla

Gap solitons in a chain of split-ring resonator dimers

Wei-na Cui [a], Hong-xia Li [a], Min Sun [a], Ling-bing Bu [b]

[a] Department of Applied Physics, Nanjing University of Science and Technology, Nanjing 210094, PR China
[b] Collaborative Innovation Center on Forecast and Evaluation of Meteorological Disasters, Key Laboratory for Aerosol-Cloud-Precipitation of China Meteorological Administration, Key Laboratory of Meteorological Disaster of Ministry of Education, Nanjing University of Information Science and Technology, Nanjing 210044, PR China

ARTICLE INFO

Article history:
Received 17 February 2017
Received in revised form 5 April 2017
Accepted 6 April 2017
Available online xxxx
Communicated by C.R. Doering

Keywords:
Gap solitons
Nonlinear
Split-ring resonator

ABSTRACT

Dynamics of a chain of split-ring resonator dimers with Kerr nonlinear interaction are investigated. A dimer is built as a pair of coupled split-ring resonators with different size. It is shown that the gap solitons with frequency lying in the gap exist due to the interaction of the discreteness and nonlinearity. Such localized structures are studied in the phase plane and analytical and numerical expressions are also obtained.

1. Introduction

The gap solitons, i.e., collective nonlinear excitations which can exist in spectrum gaps forbidden for linear waves, have been studied intensively in various physical systems [1,2]. The emergence of metamaterials in recent years add new interest to this topic. Metamaterials consist of periodically arranged meta-atoms, such as the split-ring resonators (SRRs) or other types of subwavelength resonant elements with tailored magnetic and electric responses [3,4]. A standard theoretical approach for analyzing the properties of metamaterials is based on the effective medium approximation [5]. On the other hand, metamaterials demonstrate their discrete nature with finite size as well as with larger wave vectors, and coupling effect between neighboring resonant elements is important, so they should be described as one-, two-, or three-dimensional lattices [6–9]. Magnetoinductive (MI) waves were proved to exist on SRRs arrays due to magnetic coupling between individual magnetic meta-atoms studied extensively [10–12]. Tailoring the dispersion properties opens up the possibility to manipulate guiding properties in the near field. The controllable parameters of each engineering elements provide considerably more freedom in designing the near-field behavior and, hence, in controlling the propagation of MI waves at the specified frequencies. Applications of MI waves have been reported for delay lines, phase shifters, and microwave lenses [13–15]. In linear theory, the magnetoinductive waves can not propagate and will be damped when the frequency lies in the gap of the linear spectrum. However, if the nonlinearity is considered, the results would be different. Embedding meta-atoms into nonlinear host media provides strong nonlinear response particularly for THz, infrared, and optical resonant elements [16–20]. Due to the combination of nonlinearity and discreteness in metamaterials arrays, the gap solitons or other localized modes may exist with the nonlinear frequency shifted into the linear spectrum gap. Recently, the diatomic SRRs chain comprising two different size meta-atoms per unit cell is introduced and there are two branches of magnetoinductive waves [21–24]. We have studied the nonlinear excitations in the diatomic SRRs chain, soliton excitations are considered for two different modes separately, and a nonlinear Schrödinger equation is derived to describe the envelope solitons [24]. In the following, we will study the nonlinear coupled modes and pay much attention on the soliton excitations in the vicinity of the gap of the linear spectrum. The evolution of these localized structures is studied in the phase plane and their analytical and numerical results are also proposed.

2. Physical model

The physical model we consider in the paper is the nonlinear diatomic chain of SRRs with its nearest-neighbors interaction shown in Fig. 1. We take the dimer, two elements with different size coupled to each other, as the unit to form the diatomic chain. The self-inductance, Ohmic resistance and capacitance is L_1, R_1, C_1 for the bigger SRR, but for the smaller SRR is L_2, R_2, C_2. The neighboring SRR centers has the same distance, and the period a is a fundamental physical parameter. The nearest-neighbors

E-mail address: cuiweinaa@163.com (W.-n. Cui).

http://dx.doi.org/10.1016/j.physleta.2017.04.007
0375-9601/

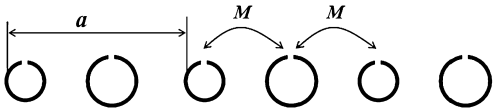

Fig. 1. Schematic of the chain of SRR dimers with nearest-neighbors interaction.

interaction between the magnetic elements is dominated by mutual inductance M. If one fills the gap of each SRRs Kerr dielectric the units show their nonlinear properties [16,25]. The equivalent permittivity $\epsilon(|E|^2) = \epsilon_0(\epsilon_l + \alpha|E|^2/E_c^2)$ depends on the electric field E, where ϵ_0 and ϵ_l represent the vacuum permittivity and linear permittivity respectively, E_c is a characteristic electric field, and $\alpha = +1$ ($\alpha = -1$) accounts for self-focusing (defocusing) nonlinearity. The SRRs have a field-dependent capacitance $C_{nj}|E|^2 = \epsilon(|E_{gj}|^2)A_j/d_{gj}$, where $j = 1, 2$ accounts for two different kinds of SRRs. E_{gj} is the electric field induced along the SRR slit. A_j and d_{gj} are the area of the cross section and the size of the slit of the SRR respectively. The charge Q_n and q_n stored in the capacitor of the big and small SRR can be obtained as

$$Q_n = C_1(1+\alpha\frac{U_n^2}{3\epsilon_l U_{c1}^2})U_n, \quad q_n = C_2(1+\alpha\frac{u_n^2}{3\epsilon_l U_{c2}^2})u_n \tag{1}$$

where $U_n = d_{g1}E_{g1}$ and $u_n = d_{g2}E_{g2}$ are the voltage across the slit of the SRRs, $C_j = \epsilon_0\epsilon_l(A_j/d_{gj})$ is the linear capacitance, and $U_{cj} = d_{gj}E_c$ ($j = 1, 2$). Neighboring SRRs are coupled due to magnetic dipole–dipole interaction through their mutual inductance M, which decays as the cube of the distance. For weak coupling between SRRs in a planar configuration, it is a good approximation to consider only nearest neighboring SRR interactions. Considering the only nearest neighboring SRR interactions, the dynamics charge of Q_n (q_n) and the current I_n (i_n) circulating in nth bigger SRR and smaller SRR can be described by

$$i_n = \frac{dq_n}{dt} \tag{2}$$

$$I_n = \frac{dQ_n}{dt} \tag{3}$$

$$L_1\frac{dI_n}{dt} + R_1 I_n + f(Q_n) + M(\frac{di_n}{dt} + \frac{di_{n+1}}{dt}) = \mathcal{E}_1(t) \tag{4}$$

$$L_2\frac{di_n}{dt} + R_2 i_n + f(q_n) + M(\frac{dI_n}{dt} + \frac{dI_{n-1}}{dt}) = \mathcal{E}_2(t) \tag{5}$$

where $\mathcal{E}_1$ and $\mathcal{E}_2$ are related to the electromotive force induced in each SRR due to the applied field, and $U_n = f(Q_n)$, $u_n = f(q_n)$ can be given implicitly from Eq. (1) by making a Taylor expansion to cubic terms. Making the translation: $t \to \omega_1 t$, $I_n \to I_c I_n$, $i_n \to i_c i_n$, $Q_n \to Q_c Q_n$, $q_n \to q_c q_n$, $\mathcal{E}_1 \to \mathcal{E}_1 U_{c1}$, $\mathcal{E}_2 \to \mathcal{E}_2 U_{c2}$, with $\omega_1^{-2} = L_1C_1$, $\omega_2^{-2} = L_2C_2$, $Q_C = C_1U_{c1}$, $q_c = C_2U_{c2}$, $I_C = U_{c1}\omega_1 C_1$, $i_c = U_{c2}\omega_2 C_2$, Eqs. (4) and (5) can be normalized to

$$\frac{d^2}{dt^2}(\lambda_1 q_n + Q_n + \lambda_1 q_{n+1}) + Q_n - \frac{\alpha}{3\epsilon_l}Q_n^3 = -\gamma_1\frac{dQ_n}{dt} + \mathcal{E}_1(t), \tag{6}$$

$$\frac{d^2}{dt^2}(\lambda_2 Q_n + q_n + \lambda_2 Q_{n-1}) + \lambda q_n - \frac{\alpha}{3\epsilon_l}q_n^3 = -\gamma_2\frac{dq_n}{dt} + \mathcal{E}_2(t), \tag{7}$$

with $\lambda_1 = Mi_c/(L_1I_c)$, $\lambda_2 = MI_c/(L_2i_c)$, $\lambda = (I_cL_1U_{c1})/(i_cL_2U_{c2})$, $\gamma_1 = R_1/(L_2\omega_1)$, $\gamma_2 = R_2/(L_2\omega_1)$. γ_1, γ_2 are the loss coefficient, which is usually very small ($\gamma_1, \gamma_2 << 1$), may account for both Ohmic and radiative losses. The magnetic interaction coefficients

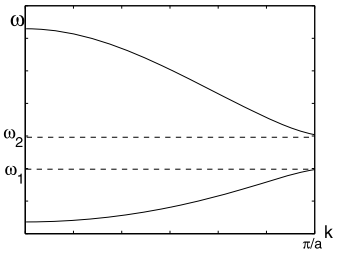

Fig. 2. Dispersion curves in the diatomic chain of SRRs.

λ_1 and λ_2 between nearest neighbors are related to the mutual inductance M. For planar configurations because the magnetic field originating in a SRR changes its direction when crossing its neighbors, λ_1 and λ_2 are negative, but for axial configurations λ_1 and λ_2 are positive. The parameter λ denotes the difference between the big SRR and small SRR. Here, we define $\lambda > 1$ without loss of generality. In the following we neglect losses and electromotive forcing by setting $\gamma_1 = \gamma_2 = 0$, $\mathcal{E}_1 = \mathcal{E}_2 = 0$. The dispersion relation of Eqs. (6) and (7) for linear waves has two different branches

$$\omega_\pm^2 = \frac{(\lambda+1) \pm \{(\lambda+1)^2 - 4\lambda[1-2\lambda_1\lambda_2(1+\cos ka)]\}^{1/2}}{2-4\lambda_1\lambda_2(1+\cos ka)}, \tag{8}$$

where ω and k are the wave frequency and wave number, the minus corresponds to the low frequency mode, and the plus corresponds to the high-frequency mode. The dimer has two discrete resonant frequencies, but for the chain made up by these dimers, each frequency will spread into a band shown in Fig. 2. There is a stop band between the two pass bands at the Brillouin-zone edge with the wave number $k = \pi/a$. The width of the frequency gap is $\Delta\omega = \omega_2 - \omega_1 = \sqrt{\lambda} - 1$ with $\omega_+(\pi/a) \equiv \omega_2 = \sqrt{\lambda}$ and $\omega_-(\pi/a) \equiv \omega_1 = 1$. When the difference between two type of SRRs decrease, i.e., $\lambda \to 1$, the system becomes monatomic lattice, the frequencies ω_1 and ω_2 coincide, and the gap in the linear spectrum disappears. The most interesting point of the spectrum is the $k = \pi/a$ where there are a pair of equivalent oscillate eigenmodes. Near the point ω_1 at the lower branch, there are no current in the small SRRs and the current in the big ones circulate with the opposite phases, or vice versa, there are no current in the big SRRs and the current in the small ones circulate with the opposite phases near ω_2. In the linear limit, the two modes are exactly decoupled at $k = \pi/a$. However, considering the nonlinear interaction, the two modes at $k = \pi/a$ can be coupled and allow localized structures with the frequencies lying in the gap.

3. Gap soliton solutions

In the vicinity of the point $k = \pi/a$, we make the ansatz [26,27]

$$Q_n = (-1)^n[V(\xi_n, \tau)\exp(i\omega_1 t) + V^*(\xi_n, \tau)\exp(-i\omega_1 t)], \tag{9}$$

$$q_n = (-1)^n[W(\xi_n, \tau)\exp(i\omega_1 t) + W^*(\xi_n, \tau)\exp(-i\omega_1 t)], \tag{10}$$

where $\xi_n = \varepsilon^2 na$, $\tau = \varepsilon^2 t$ are slow variables, ε is a small parameter, and ω_1 is the largest frequency of the lower branch (the lower frequency of the gap). Assuming that the functions $V(\xi_n, \tau)$ and $W(\xi_n, \tau)$ are slowly varying in space and time, and making the rotating-wave approximation, we may obtain the following two-coupled equations from Eqs. (6) and (7) retaining to order $O(\varepsilon^3)$

$$i\omega_1\frac{\partial V}{\partial t} + \lambda_1 a\omega_1^2\frac{\partial W}{\partial x} - \frac{\alpha}{2\epsilon_l}|V|^2 V = 0, \tag{11}$$

$$i\omega_1\frac{\partial W}{\partial t} - \lambda_2 a\omega_1^2\frac{\partial V}{\partial x} + \Delta\omega^2 W - \frac{\alpha}{2\epsilon_l}|W|^2 W = 0, \tag{12}$$

where the variable $x = na$ is treated as continuous one and $\Delta\omega^2 = \omega_2^2 - \omega_1^2$. The coupling effect between the two modes is exhibited

by the derivative terms in Eqs. (11) and (12). To analyze the localized structures in the framework of the system (11) and (12), we look for stationary solutions in the form

$$V = f_1(x)e^{-i\Omega t}, \quad W = f_2(x)e^{-i\Omega t}, \tag{13}$$

where Ω is an arbitrary real parameter and f_1 and f_2 is real. The stationary solutions for f_1 and f_2 are described by the system of two ordinary differential equations

$$\frac{df_1}{dx} = -\Delta_1 f_2 + \nu_1 f_2^3, \tag{14}$$

$$\frac{df_2}{dx} = \Delta_2 f_1 - \nu_2 f_1^3, \tag{15}$$

with $\Delta_1 = -2(\Delta\omega^2 + \omega_1\Omega)/(\lambda_2\omega_1^2 a)$, $\nu_1 = -\alpha/(\epsilon_l\lambda_2\omega_1^2 a)$, $\Delta_2 = -2\Omega/(\lambda_1\omega_1 a)$, $\nu_2 = -\alpha/(\epsilon_l\lambda_1\omega_1^2 a)$. It is not difficult to get a conservative quantity of Eqs. (14) and (15),

$$E = 2\Delta_2 f_1^2 + 2\Delta_1 f_2^2 - \nu_2 f_1^4 - \nu_1 f_2^4. \tag{16}$$

Thus Eqs. (14) and (15) describe the dynamics of a Hamiltonian system with one degree of freedom. The exact solution can be obtained by introducing an auxiliary function $g = f_1/f_2$, which satisfies

$$(\frac{dg}{dx})^2 = (\Delta_1 + \Delta_2 g^2)^2 - E(\nu_1 + \nu_2 g^4). \tag{17}$$

Then f_1, f_2 may be found by the relation

$$f_2^2 = \frac{1}{\nu_1 + \nu_2 g^4}\{(\Delta_1 + \Delta_2 g^2) \pm [(\Delta_1 + \Delta_2 g^2) - E(\nu_1 + \nu_2 g^4)]^{1/2}\}, \tag{18}$$

$$f_1 = g f_2. \tag{19}$$

Different kinds of solutions, including localized ones, are characterized by different values E, as well as by the parameters Δ_1, Δ_2, ν_1 and ν_2. Phase diagram provide us a visible method to analyze the possible solutions of Eqs. (14) and (15), where different kinds localized modes correspond to separatrix curves. In the following, we analyze the critical points and separatrixes on the phase plane (f_1, f_2), and pay much attention on the critical points decided by the signs of the parameters Δ_1, Δ_2, ν_1 and ν_2.

For $\mathrm{sgn}(\Delta_1\Delta_2) < 0$ and $\mathrm{sgn}(\Delta_j\nu_j) > 0$ $(j = 1, 2)$, there are three fixed points in the phase plane as the dynamical system (14) and (15) shown. The localized structures are possible corresponding to the separatrix curves. At the same time, we note the configurations of the lattice can be obtained from (9), (10), and (13) as

$$Q_n = (-1)^n[f_1 e^{i(\omega_1 - \Omega)t} + c.c.] = (-1)^n[f_1 e^{i\omega' t} + c.c.], \tag{20}$$

$$q_n = (-1)^n[f_2 e^{i(\omega_1 - \Omega)t} + c.c. = (-1)^n[f_2 e^{i\omega' t} + c.c.], \tag{21}$$

where the variation frequency of current in SRRs is $\omega' = \omega_1 - \Omega$. If the conditions $\Omega < 0$ and $|\Omega| < \omega_2 - \omega_1$ are satisfied, the oscillatory frequency ω' lies in the gap $\Delta\omega = \omega_2 - \omega_1$ which the linear waves cannot propagate. However, the waves with frequency in the gap maybe exist in the form of localized modes, which are called gap solitons. For the planar configuration with $\lambda_1 < 0$ and $\lambda_2 < 0$, the parameters $\Delta_2 < 0$ and $\Delta_1 > 0$ for $\Omega < 0$. If the embedded medium is self-focusing medium $\alpha > 0$, $\nu_1 > 0$, the system possesses a saddle point at $(0, 0)$, and two centers at $[0, \pm(\Delta_1/\nu_1)^{1/2}]$ as sketched in Fig. 3. The localized structures with frequency $\omega_1 < \omega' < \omega_2$ in the frequency gap are found. The separatrixes OAB and OCD (homoclinic orbits) shown on the phase plane (f_1, f_2) correspond to the gap solitons, and the numerical solutions are also shown in Figs. 4(a) and 4(b). We can see the envelope of the small

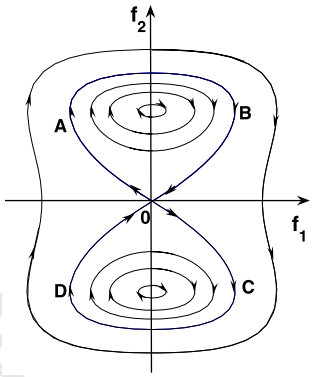

Fig. 3. The phase diagram for $\lambda_1 < 0$, $\lambda_2 < 0$, $\alpha > 0$, and $\Omega < 0$.

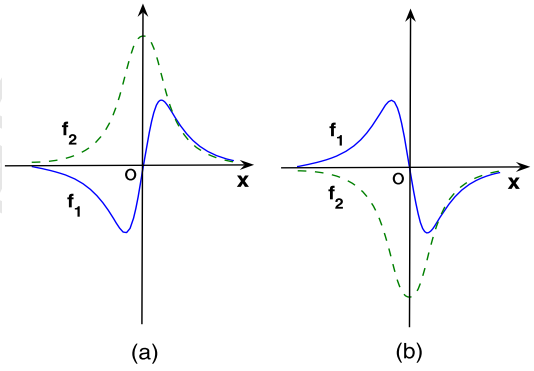

Fig. 4. (a) The solution corresponding to the homoclinic orbit OAB in Fig. 3; (b) The solution corresponding to the homoclinic orbit OCD in Fig. 3.

SRRs f_2 has the shape of standard solitons, but the big SRRs f_1 has the shape different from the standard envelope solitons. To find the analytical solutions corresponding to the gap solitons we note that the separatrix curves on the phase plane correspond to $E = 0$. The boundary condition for g is $|g| = \infty$ for $x = 0$ and $|g| = \infty$ for $x = \pm\infty$. Integrating Eq. (17) yields the exact solution

$$g = \pm(-\Delta_1/\Delta_2)^{1/2}\coth[\pm\,\Delta_2\,(\Delta_1/\Delta_2)^{1/2}x], \tag{22}$$

$$f_2 = \delta[2\frac{\Delta_1}{\nu_1}\frac{1 - \coth^2(\beta x)}{1 + \nu_2\Delta_1^2/(\nu_1\Delta_2^2)\coth^4(-\Delta_1 x)}]^{1/2}, \tag{23}$$

$$f_1 = g f_2, \tag{24}$$

with $\delta = \pm 1$. $\delta = +1(-1)$ corresponds to the OAB (OCD) orbit. On the other hand, the gap solitons with frequency $\omega_1 < \omega' < \omega_2$ similar to the above solutions are also exist in the axial configuration case with $\lambda_1 > 0$ and $\lambda_2 > 0$, and for self-defocusing medium $\alpha < 0$.

In another case for $\mathrm{sgn}(\Delta_1\Delta_2) > 0$ and $\mathrm{sgn}(\Delta_j\nu_j) > 0$ $(j = 1, 2)$, there also exist localized soliton solutions for $\Omega > 0$, but the wave frequency $\omega' = \omega_1 - \Omega$ lies below the gap of the linear spectrum. The phase portraits of the dynamical system have been shown in Fig. 5 with $\lambda_1 < 0$, $\lambda_2 < 0$ and $\alpha > 0$. It is shown there are nine fixed points in the phase plane. The fixed points $(0, 0)$ and $[\pm(\Delta_2/\nu_2)^{1/2}, \pm(\Delta_1/\nu_1)^{1/2}]$ are centers, and $[0, \pm(\Delta_1/\nu_1)^{1/2}]$ and $[\pm(\Delta_2/\nu_2)^{1/2}, 0]$ are saddle points. We pay much attention on the separatrix curves connecting a pair of the neighboring saddle points, which correspond to soliton or kink solutions. There are two different types of separatrix curves. One is the ABC type (heteroclinic) orbit and the other is the EFE type (homoclinic) orbit (see Fig. 5). The numerical solutions for f_1 and f_2 are obtained shown in Fig. 6. We can also obtain exact and explicit solutions corresponding to these separatrixes. For ABC type, the solutions f_1

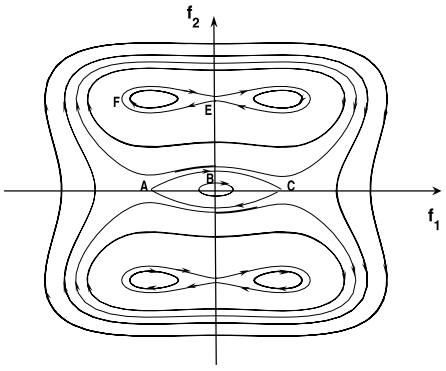

Fig. 5. The phase diagram for $\lambda_1 < 0$, $\lambda_2 < 0$, $\alpha > 0$, and $\Omega > 0$.

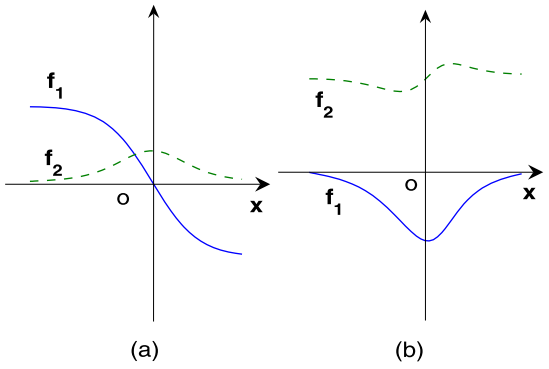

Fig. 6. (a) The solution corresponding to the heteroclinic orbit ABC in Fig. 5; (b) The solution corresponding to the homoclinic orbit EFE in Fig. 5.

and f_2 are relevant to the heteroclinic orbit from $[-(\triangle_2/\nu_2)^{1/2}, 0]$ to $[(\triangle_2/\nu_2)^{1/2}, 0]$. The boundary condition for g is $|g| = \infty$ for $x = \pm\infty$ and $|g| = \infty$ for $x = 0$. Equation (17) may be easily integrated to give the solution

$$g = \pm\frac{\beta_1}{\beta_2}\frac{1}{\sinh(\beta_1 x)}, \tag{25}$$

$$f_2^2 = \frac{1}{\nu_1 + \nu_2 g^4}\{(\Delta_1 + \Delta_2 g^2) \pm \beta_1|g|[g^2 + (\beta_2/\beta_1)^2]^{1/2}\}, \tag{26}$$

$$f_1 = g f_2, \tag{27}$$

with $\beta_1 = \beta_2^2/(\Delta_2^2 - \Delta_1^2\nu_2/\nu_1)^{1/2}$ and $\beta_2 = (2\Delta_1\Delta_2)^{1/2}$. For EFE type, if the orbits pass the saddle points $[0, \pm(\triangle_1/\nu_1)^{1/2}]$, one have $E = \Delta_1^2/\nu_1$. The boundary condition is $|g| = \infty$ for $x = \pm\infty$ and $|g| = \text{const}$ for $x = 0$, the solution is

$$g = \pm[\Delta_1/\Delta_2 - \sigma_1\Delta_2/(\sigma_2\Delta_1)]^{1/2}/\sqrt{2}\cosh(\beta_1 x), \tag{28}$$

$$f_2^2 = \frac{1}{\nu_1 + \nu_2 g^4}\{(\Delta_1 + \Delta_2 g^2) \pm \beta_1[g^2 - (\beta_2/\beta_1)^2\nu_1/\nu_2]^{1/2}\}, \tag{29}$$

$$f_1 = g f_2. \tag{30}$$

We can see the solitons and noncutoff kink solutions are both possible corresponding to the separatrixes ABC and EFE. Such localized modes are original from the balance between the effect of nonlinearity and dispersion due to the periodic location of SRRs. The soliton lattice pattern corresponding to the separatrix OAB in Fig. 3 and ABC in Fig. 5 are shown in Fig. 7. It can be seen that the localized nonlinear magnetoinductive waves have a spatial extension, and the current in each SRRs oscillates with their own amplitude.

Since gap solitons as one of localized structures was first introduced by Chen and Mills in 1987 [1], families of gap solitons

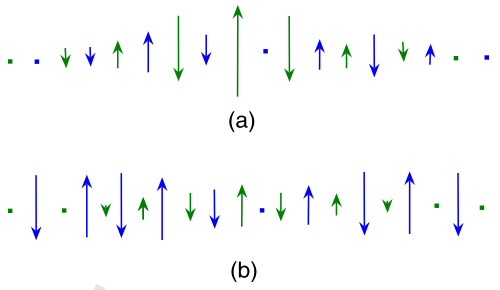

Fig. 7. (a) The gap soliton lattice pattern corresponding to the separatrix OAB in Fig. 3; (b) The soliton lattice pattern corresponding to the separatrix ABC in Fig. 5.

were analyzed in different nonlinear system. Considering magnetic metamaterials composed of SRRs can be controlled by adjusting the size and distance between them artificially, nonlinear chain of SRR dimers can be taken as good candidate to display gap solitons. For the experimental SRRs array system, one can choose singly split ring as the resonant elements similar to those in Ref. [28]. The analytical expressions for the resonant frequency of such single ring SRR is $\omega_s = 1/\sqrt{LC}$. The self-inductance is $L = L_{mag} + L_{kin}$ with magnetic inductance $L_{mag} = \mu_0 r\{\log[8r/(h+w)] - 1/2\}$ and kinetic inductance $L_{kin} = (2\pi r - g)/(S\omega_p^2\varepsilon_0)$. The total capacitance C is the sum of the surface capacitances $C_{surf} = 2\varepsilon_0(h+w)/\pi\log(4r/g)$ and the gap capacitances $C_{gap} = \varepsilon_0 hw/g + \varepsilon_0(h+g+w)$ with the mean radius r, the height h, the width w, and the gap width g, where ω_p is the plasma frequency, S is the area of the ring's cross section. If the parameters are taken as $w = 0.1r$, $h = r$, $g = 0.1r$, the resonant frequency SRR is about 57.7 THz for $r = 0.3$ μm and 82.3 THz for $r = 0.2$ μm [28]. It is appropriate to choose the linear permittivity $\epsilon_l = 2$ and the parameter relating to the gap size as $\lambda = 1.2$. For planar geometry the coupling parameters can be taken as $\lambda_1 = -0.12$, $\lambda_2 = -0.15$ [6]. For silver made SRRs, whose conductivity and skin depth are $\sigma = 6.15 \times 10^7$ S/m and $\delta \sim 20$ nm, respectively, we obtain $R = 2a/\sigma h\delta \simeq 3.44$ and $\gamma \simeq 0.01$. The great flexibility of metamaterial engineering provide an alternative way of generating gap solitons in experiment.

4. Conclusions

In conclusion, we have investigated the nonlinear localized structures in a chain of SRR dimers with Kerr nonlinearity. The results show that the gap solitons may exist in this system when the soliton frequency lies within the gap. An experiment for observing the gap solitons in the SRR dimers chain is also suggested. We believe that these results may be useful for the further study of the nonlinear properties in magnetic metamaterials.

Acknowledgements

This work was financially supported by the National Natural Science Foundation of China (Grant No. 41675133) and the Natural Science Foundation of Jiangsu Province (Grant No. BK20141480 and Grant No. BE2015003-4).

References

[1] W. Chen, D.L. Mills, Phys. Rev. Lett. 58 (1987) 160.
[2] Y.S. Kivshar, G.P. Agrawal, Optical Solitons: From Fibers to Photonic Crystals, Academic, San Diego, 2003.
[3] D.R. Smith, J.B. Pendry, M.C.K. Wiltshire, Science 305 (2004) 788.
[4] N.I. Zheludev, Science 328 (2010) 582.
[5] G.V. Eleftheriades, K.G. Balmain, Negative-Refraction Metamaterials: Fundamental Principles and Applications, Wiley-IEEE Press, Hoboken, 2005.
[6] O. Sydoruk, A. Radkovskaya, O. Zhuromskyy, E. Shamonina, M. Shamonin, Phys. Rev. B 73 (2006) 224406.

[7] H. Liu, D.A. Genov, D.M. Wu, Y.M. Liu, J.M. Steele, C. Sun, S.N. Zhu, X. Zhang, Phys. Rev. Lett. 97 (2006) 243902.
[8] M. Beruete, F. Falcone, M.J. Freire, R. Marqués, J.D. Baena, Appl. Phys. Lett. 88 (2006) 083503.
[9] W.N. Cui, Wen Lu, H.X. Li, S.M. Liu, Y.Y. Zhu, Opt. Commun. 367 (2016) 346.
[10] E. Shamonina, V.A. Kalinin, K.H. Ringhofer, L. Solymar, Electron. Lett. 38 (2002) 371.
[11] E. hamonina, V.A. Kalinin, K.H. Ringhofer, L. Solymar, J. Appl. Phys. 92 (2002) 6252.
[12] N. Lazarides, V. Paltoglou, G.P. Tsironis, Int. J. Bifurc. Chaos Appl. Sci. Eng. 21 (2011) 2147.
[13] M.J. Freire, R. Marques, F. Medina, M.A.G. Laso, F. Martin, Appl. Phys. Lett. 85 (2004) 4439.
[14] I.S. Nefedov, S.A. Tretyakov, Microw. Opt. Technol. Lett. 45 (2005) 98.
[15] M.J. Freire, R. Marques, Appl. Phys. Lett. 86 (2005) 182505.
[16] A.A. Zharov, I.V. Shadrivov, Y.S. Kivshar, Phys. Rev. Lett. 91 (2003) 037401.
[17] M. Lapine, I.V. Shadrivov, Y.S. Kivshar, Rev. Mod. Phys. 86 (2014) 1093.
[18] Z.Y. Bai, G.X. Huang, L.X. Liu, S. Zhang, Sci. Rep. 5 (2015) 13780.
[19] Q. Zhang, C.H. Tan, G.X. Huang, Sci. Rep. 6 (2016) 21143.
[20] Z.Y. Bai, G.X. Huang, Phys. Rev. A 93 (2016) 013818.
[21] O. Sydoruk, O. Zhuromsky, E. Shamonina, Appl. Phys. Lett. 87 (2005) 072501.
[22] M.I. Molina, N. Lazarides, G.P. Tsironis, Phys. Rev. E 80 (2009) 046605.
[23] N. Lazarides, G.P. Tsironis, Phys. Rev. Lett. 110 (2013) 053901.
[24] W.N. Cui, Y.Y. Zhu, H.X. Li, S.M. Liu, Phys. Rev. E 81 (2010) 016604.
[25] N. Lazarides, M. Eleftheriou, G.P. Tsironis, Phys. Rev. Lett. 97 (2006) 157406.
[26] Y.S. Kivshar, N. Flytzanis, Phys. Rev. A 46 (1992) 7972.
[27] G.X. Huang, J. Shen, H.J. Quan, Phys. Rev. B 48 (1993) 16795.
[28] V. Delgado, O. Sydoruk, E. Tatartschuk, R. Marques, M.J. Freire, L. Jelinek, Metamaterials 3 (2009) 57.

Please cite this article in press as: W.-n. Cui et al., Gap solitons in a chain of split-ring resonator dimers, Phys. Lett. A (2017), http://dx.doi.org/10.1016/j.physleta.2017.04.007